

## Defects and Impurities at the Si/Si(100) Interface Studied with Monoenergetic Positrons

Peter J. Schultz and E. Tandberg

*Department of Physics, The University of Western Ontario,  
London, Ontario, Canada N6A 3K7*

K. G. Lynn and Bent Nielsen

*Brookhaven National Laboratory, Upton, New York 11973*

and

T. E. Jackman, M. W. Denhoff, and G. C. Aers

*Microstructural Sciences Laboratory, National Research Council of Canada,  
Ottawa, Ontario, Canada K1A 0R6*

(Received 21 March 1988)

Positrons implanted with varying energies (0–20 keV) have been used to study silicon epilayers grown by molecular-beam epitaxy on Si(100) substrates. Defects at the initial growth interface and throughout the overlayer have been observed and depth profiled. In addition, field-driven positron drift observed in some of the epilayers is shown to be consistent with estimated concentrations of (active) interfacial impurities. The study demonstrates that positrons can be used *nondestructively* to profile structural defects and electric fields in thin films and at interfaces.

PACS numbers: 68.35.Dv, 68.55.Bd, 78.70.Bj

Molecular-beam epitaxy (MBE) is now extensively used for creating group-IV multilayer structures. The composition of these superlattices can be tailored to produce structures with specific physical or electronic properties.<sup>1</sup> As in any growth process, impurities, dislocations, or other types of structural defects formed in the overlayers can have a detrimental effect on the electronic properties of the material. The origin and consequence of damage in artificially grown semiconductors is an area of intense study, even though there are relatively few ways to profile buried defects in dilute quantities.<sup>2–4</sup> In the last few years, several studies have demonstrated that positrons implanted with varying energies can be used to study defects nondestructively in the near-surface region of solids.<sup>5–10</sup> In the present Letter, we report on the first results of a study of the properties of MBE-grown Si/Si(100) epilayers (single layer). The data show that positrons are sensitive to some types of structural defects concentrated at the initial growth interface and distributed throughout the overlayer of some Si/Si(100) samples. The data also show evidence of electric-field-induced positron mobility, which can be directly attributed to active impurities known to be at the interface.

The epilayers were grown at  $\approx 700^\circ\text{C}$  without intentional doping to a thickness of  $\approx 3000 \text{ \AA}$  at a rate of  $\approx 3 \text{ \AA/s}$ . Substrates were prepared by growth of an *ex situ* sacrificial oxide in an ultraviolet/ozone reactor which was removed by heating to  $\approx 900^\circ\text{C}$  for 5 min, followed by 10 min at the same temperature with a low ( $< 0.1 \text{ \AA/s}$ ) Si flux.<sup>11</sup> Two positron beams were used to study the epilayers, which provide beams of monoenergetic positrons ( $\approx 10^4$  to  $10^6 e^+/s$ ) that are tunable from near

0 to several tens of kiloelectronvolts. These facilities are described elsewhere,<sup>12,13</sup> and studies of solids with variable-energy positrons (including details of the analysis summarized below) are reviewed by Schultz and Lynn.<sup>14</sup>

The depth distribution or profile of positrons implanted into a monatomic material such as Si can be approximated by the derivative of a Gaussian,<sup>7,15</sup> with a mean depth (in microns) of

$$\bar{z} = (0.04/\rho)E^{1.6}, \quad (1)$$

where  $\rho \text{ gm/cm}^3$  is the mass density of the target and  $E$  keV is the incident positron energy. Once thermalized, the positrons diffuse through the solid, annihilating from this *freely diffusing* state, or after being trapped in bulk-defect or surface localized states. When a positron annihilates with an electron, the 511-keV  $\gamma$  rays are Doppler broadened because of the finite momentum of the annihilation pair. This distribution is measured with two different high-resolution intrinsic Ge detectors (resolution  $< 1.5 \text{ keV}$  at 511 keV) and is characterized by the "S parameter,"<sup>14</sup> defined as the integral of a central fixed portion of the annihilation line normalized by the total intensity.

The probability of positron annihilation from various states can be predicted by the steady-state diffusion-annihilation equation,<sup>14</sup> which is given (in one dimension) by

$$D + \partial^2 n(z)/\partial z^2 - [\lambda_B + \nu C(z)]n(z) - \partial v_d n(z)/\partial z + P(z) = 0, \quad (2)$$

where  $n(z)$  is the positron density as a function of depth,

$P(z)$  is the time-independent "initial" depth profile of positrons (i.e., constant source),  $D_+$  is the positron diffusion coefficient,  $\lambda_B$  is the bulk-positron annihilation rate ( $\approx 4.5 \times 10^9/s$ ), and  $v_d$  is the field-dependent drift-velocity given by  $v_d = \mu E$  (the mobility  $\mu = 60 \text{ cm}^2/V/s$ ).<sup>16</sup> In practice one includes only one type of defect in the solid with an atomic concentration  $C(z)$  and a specific trapping rate,  $\nu$ . Depth distributions of more than one type of defect are presently difficult to resolve with this technique.

If there are no defects which trap positrons [i.e.,  $C(z)=0$ ] the diffusion equation (2) may be solved analytically. In this case the mean diffusion length  $L_+$  is related to  $D_+$  by

$$L_+ = [D_+/\lambda_B]^{1/2}. \quad (3)$$

It turns out that Eq. (3) applied even when defect trapping and/or electric fields influence the positron's motion, so long as these effects do not vary with depth in the sample. In such cases,  $\lambda_B$  must be replaced by an "effective" annihilation rate,  $\lambda_{\text{eff}}$ .<sup>17</sup> If there are *nonuniform* effects, one must numerically simulate the positron motion as a function of incident energy by numerically solving the diffusion equation (2) including (where necessary) positron drift velocity and a (depth) profile of defects. In this step, all quantities in Eq. (2) are treated as "known" (or assumed), and the output parameters are the relative fractions of positrons which annihilate while free in the bulk ( $F_B$ ), while trapped at defects ( $F_D$ ), or while trapped at the surface ( $F_S$ ). These contribute linearly to the measured line shape for each incident positron energy,  $E$ :

$$S_{\text{measured}} = F_B S_B + F_D S_D + F_S S_S, \quad (4)$$

where  $S_S/S_B$  and  $S_D/S_B$  are independent parameters derived from a least-square fit to the parametrized data.

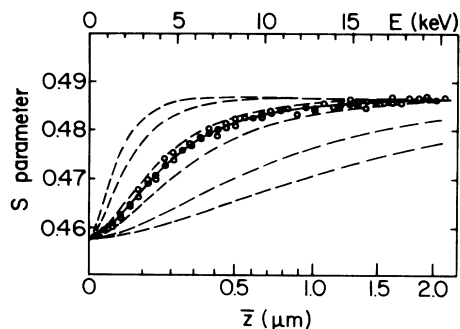


FIG. 1. Doppler broadening line shape ( $S$  parameter) vs incident positron energy (upper scale) or mean "stopping" depth,  $\bar{z}$  [Eq. (1)]. Data are shown for Cz-Si(100) bulk material. The solid curve is fitted to the data on the assumption of no defects or electric-field effects, and the dashed curves show the effect of uniform fields ( $10^3$ ,  $5 \times 10^3$ , and  $10^4$  V/cm) directed into the bulk (upper three) and out towards the surface (lower three).

This technique is similar to the analysis discussed elsewhere,<sup>7,8</sup> with the difference that electric-field effects are included.<sup>18</sup>

Figure 1 shows data for a "defect-free"  $p$ -type (boron) Czochalski-grown (Cz-) Si(100) crystal. The results of the analytical fit to the data are also indicated in the figure by the solid line ( $L_+ \approx 2150 \text{ \AA}$  and  $D_+ \approx 2.1 \pm 0.2 \text{ cm}^2/s$ ). Similar results were obtained for  $n$ -type (phosphorus) Cz-Si (typical carrier concentration  $\approx 10^{15} \text{ cm}^{-3}$ ;  $\approx 4-9 \text{ } \Omega\text{-cm}$ ). The value of  $D_+ = 2.1 \text{ cm}^2/s$  was used for all analysis of 300-K data for MBE-grown epilayers. For FZ-Si(100) (FZ denotes float-zone refined) we observed longer diffusion lengths ( $L_+ \approx 2450 \text{ \AA}$ ;  $D_+ \approx 2.7 \pm 0.2 \text{ cm}^2/s$ ), consistent with decreased positron-impurity scattering<sup>19</sup> (for FZ-Si, carrier concentration  $\approx 10^{13} \text{ cm}^{-3}$ ;  $\approx 10^2-10^4 \text{ } \Omega\text{-cm}$ ). As with the Cz-Si(100), the value of  $L_+$  was the same for both  $n$ - and  $p$ -type FZ-Si(100).

These observations suggest that electric-field effects are very weak or negligible near the surface (i.e.,  $\leq 1 \text{ } \mu\text{m}$ ) of these bulk materials. The effect of uniform electric fields on positron back diffusion is illustrated by the dashed curves in Fig. 1, which were calculated with the assumption of relatively typical (weak) fields of between  $10^3$  and  $10^4$  V/cm. They show that a field reversal in a sample of one type relative to that of another would lead to easily observable differences in the  $S$ -vs- $E$  data.

In Fig. 2(a) we show data for an intrinsic  $0.3\text{-}\mu\text{m}$  Si epilayer grown on  $n$ -type Cz-Si(100) (triangles). These results are similar to those for the defect-free *bulk* material (represented by the dashed curve) although they are not identical. The solid curve shown in Fig. 2(a) was obtained with the assumption of *no* defects and an electric field ( $\approx 2 \times 10^3$  V/cm) originating from negative charge trapped at the interface. Electric fields of this magnitude would be predicted for boron ( $\approx 10^{11} \text{ cm}^{-2}$ )

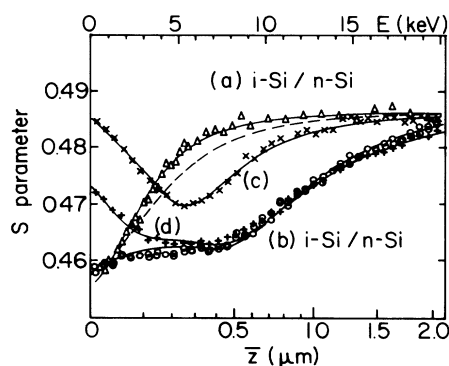


FIG. 2. Intrinsic Si epilayers grown on Si(100). Data are (a) the "best" obtained (i.e., showing little or no positron trapping), and (b)-(d) a sample containing oxide-type defects and electric-field effects (see text). All data are for samples at  $20^\circ\text{C}$ , except (c) which is at  $300^\circ\text{C}$ . The solid curves are obtained by our iteratively solving the diffusion equation (2), and the dashed curve is for the bulk material (Fig. 1).

at the interface, which is a well-known impurity at MBE-grown silicon-silicon interfaces.<sup>20</sup> In spite of the obvious quality of the fit shown in Fig. 2(a), the model is not unique. The data can also be fitted by our assuming no electric field and a uniform (dilute) concentration of defects in the overlayer ( $\nu C = 3 \times 10^9$ ;  $S_D/S_B = 1.03$ ), although the  $\chi^2$  is in this case slightly higher. By use of the specific trapping rate obtained for point defects in silicon by positron lifetime techniques<sup>21,22</sup> ( $\nu \approx 3 \times 10^{14} \text{ s}^{-1}$ ), the above implies a defect concentration of  $C \approx 10^{-5}$ . Given the systematic limitations of the present experiment (e.g., stopping-profile uncertainties, statistic, etc.), it would be difficult to rule out the latter defect-based model reliably *without* the supporting evidence discussed below.

Figure 2 also shows results obtained for an epilayer ( $\approx 0.35 \mu\text{m}$ ) grown without proper cleaning of the substrate [Fig. 2(b), circles]. The substrate was heated to a temperature slightly below  $800^\circ\text{C}$  resulting in the sacrificial oxide not being completely removed prior to overlayer growth. High-resolution TEM confirmed that the overlayer growth was epitaxial, but that irregular pockets of oxide-related defects were present at the interface. In the low-resolution TEM image in Fig. 3 the defects show up as a dark line marking the interface, which would not otherwise be observable.

Together with the as-grown ( $20^\circ\text{C}$ ) data shown in Fig. 2(b), results are also shown for the same sample measured [2(c)] at  $300^\circ\text{C}$  (crosses), and [2(d)] after returning to room temperature (plusses). The curves shown through 2(b)-2(d) are the best self-consistent fit we could achieve for all three data sets. The model assumes a relatively low defect density in the epilayer ( $\nu C = 3 \times 10^9 \text{ s}^{-1}$  for  $0 < z \leq 3450 \text{ \AA}$ ) and a higher den-

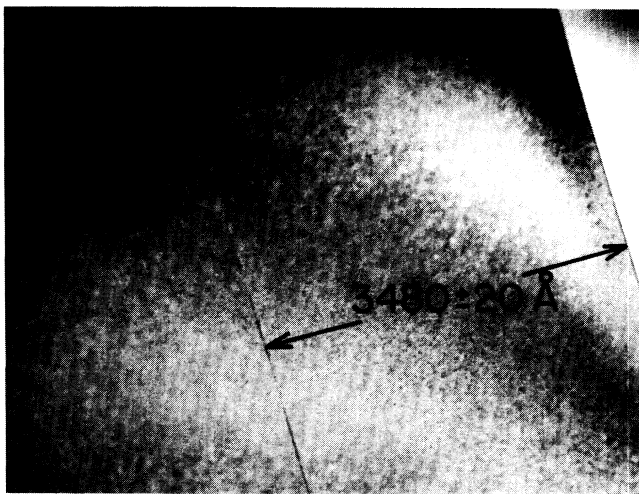


FIG. 3. Transmission micrograph of the Si/Si(100) epilayer of Fig. 2(b). The dark line is due to the oxide-type defects at the interface.

sity at the interface ( $\nu C = 1.5 \times 10^{13} \text{ s}^{-1}$  for  $3450 < z \leq 3500 \text{ \AA}$ ). An electric field of  $2 \times 10^4 \text{ V/cm}$  (towards the interface) extending from  $500 \leq z \leq 6500 \text{ \AA}$  was *required* for curves 2(b) and 2(d). This result supports the model used above for 2(a), which *included* (weaker) electric-field effects with *no* defect trapping at the interface ( $C \ll 10^{-5}$ ). The model for data in 2(c) ( $300^\circ\text{C}$ ) did not involve an electric field because of thermally activated free carriers, although the diffusion coefficient (which was  $2.1 \text{ cm}^2/\text{s}$  for all data at  $20^\circ\text{C}$ ) was  $D_+ = 0.5 \pm 0.2 \text{ cm}^2/\text{s}$ . This reduction in  $D_+$  yields a temperature dependence of  $T^{-1.6 \pm 0.4}$ . This is stronger than the  $T^{-0.5}$  predicted for positron-acoustic-phonon scattering,<sup>14</sup> but it is consistent with the  $T^{-1.3}$  obtained from hole mobility measurements<sup>19</sup> and indicates that optical-phonon scattering may be important for positron diffusion in Si. Since there is still no consensus on experimental determinations of the temperature dependence of  $D_+$ , this needs further study.

The ratio  $S_D/S_B \approx 0.93$  for all three curves, which implies that  $S_D$  is similar to the surface  $S_S$  (prior to heating; see Figs. 1 and 2 for  $S_S$  and  $S_B$ ). This is consistent with the expectation that the defects are oxide related and consistent with an independent (bulk) study of positron trapping at oxygen-related defects in Cz-Si crystals.<sup>21,22</sup> If we assume the same specific trapping rate as before ( $\nu \approx 3 \times 10^{14}$ ), our data indicate atomic concentrations of  $\approx 10^{-5}$  for the overlayer and 0.05 for the interface ( $\pm 25 \text{ \AA}$ ). Because of the coupling between  $S_D$  and  $F_D$  [Eq. (4)] it is possible that different values of  $\nu C$  would fit the data. A factor of 5 increase (decrease) of  $\nu C$  was tested which resulted in a change of  $S_D/S_B$  of only  $-1\%$  ( $+1\%$ ), but the resulting model(s) did not fit the data as well as that shown in Fig. 2. The reason  $S_S$  is larger after heating [2(c) and 2(d)] is because the surface has changed to allow positronium to form.<sup>14</sup>

In contrast to the  $S_D/S_B$  ratio deduced for this sample, we have observed  $S_D/S_B \approx 1.03-1.05$  for highly defected silicon overlayers produced by low growth temperatures.<sup>23</sup> Similar ratios were observed independently for Si crystals irradiated with high-energy ions.<sup>8</sup> Thus, it is clear that the positron annihilation characteristics for the oxide-related defect are distinct from those for open volume defects in silicon.

In conclusion, we have observed the effects of positron drift in internal fields and localization in defects at interfaces of MBE-grown Si epilayers on Si(100). The defects observed are patches of (amorphous) oxide near the interface, which remain following incomplete cleaning of the growth substrate. Bipolar electric-field intensities of  $\approx 2 \times 10^3$  to  $2 \times 10^4 \text{ V/cm}$  were required to model the data in agreement with the presence of boron impurities at the interface, as measured by secondary-ion mass spectroscopy.

The work described in this Letter represents the first step in the utilization of variable-energy positrons to

study thin Si films and their interfaces. The modeling technique is so far limited by the correlation of modeling parameters caused by systematic uncertainties. These include positron trapping rates (in various types of defects) and the positron stopping profile (which will be *particularly* important for multilayered heterostructures). However, it is already clear from the results presented here that many new and interesting studies of buried layers and interfaces in semiconductors will follow, which can benefit directly from the *nondestructive* nature of the probe. Even without the theoretical modeling of the data, the open-volume defects and electric-field effects are clearly observed in the results.

We gratefully acknowledge the assistance of J. Cole, W. N. Lennard, G. R. Massoumi, J. McCaffrey, and R. Stoner. We also acknowledge useful discussions with L. C. Feldman, L. R. Logan, and A. Vehanen. Work is supported by the Natural Sciences and Engineering Research Council of Canada (P.J.S.) and by the U.S. Department of Energy Division of Materials Sciences, Contract No. DE-AC02-76CH00016 (K.G.L.).

<sup>1</sup>J. C. Bean, *Physics Today* **39**, No. 10, 36 (1986).

<sup>2</sup>*Proceedings of the Second International Symposium on Si MBE, 1987*, edited by J. C. Bean (Electrochemical Society, New York, 1987); Y. Ota, *Thin Solid Films* **106**, 3 (1983).

<sup>3</sup>*Proceedings of the Thirteenth International Conference on Defects in Semiconductors, Coronado, California, 1984*, edited by L. C. Kimerling and J. M. Parsey, Jr. (The Metallurgical Society of American Institute of Mining, Metallurgical and Petroleum Engineers, Warrendale, PA, 1985).

<sup>4</sup>*Defects in Electronic Materials*, edited by M. Stavola, S. J. Pearton, and G. Davies, *MRS Symposia Proceedings Vol. 104* (Materials Research Society, Pittsburgh, PA, 1987).

<sup>5</sup>P. J. Schultz, K. G. Lynn, W. E. Frieze, and A. Vehanen, *Phys. Rev. B* **27**, 6626 (1983).

<sup>6</sup>K. G. Lynn, D. M. Chen, B. Nielsen, R. Pareja, and S. Myers, *Phys. Rev. B* **34**, 1449 (1986).

<sup>7</sup>A. Vehanen, K. Saarinen, P. Hautojärvi, and H. Huomo, *Phys. Rev. B* **35**, 4606 (1987).

<sup>8</sup>J. Keinonen, M. Hautala, E. Rauhala, M. Erola, J. Lahtinen, H. Huomo, A. Vehanen, and P. Hautojärvi, *Phys. Rev. B* **36**, 1344 (1987).

<sup>9</sup>A. R. Köymen, D. W. Gidley, and T. W. Capehart, *Phys. Rev. B* **35**, 1034 (1987).

<sup>10</sup>B. Nielsen, K. G. Lynn, Y-C. Chen, and D. O. Welch, *Appl. Phys. Lett.* **51**, 1022 (1987).

<sup>11</sup>M. Tabe, *Appl. Phys. Lett.* **45**, 1073 (1984); D. C. Houghton, D. J. Lockwood, M. W. C. Dharma-Wardana, E. W. Fenten, J. M. Baribeau, and M. W. Denhoff, *J. Cryst. Growth* **81**, 434 (1987).

<sup>12</sup>K. G. Lynn and H. Lutz, *Rev. Sci. Instrum.* **51**, 977 (1980); K. G. Lynn, B. Nielsen, and J. H. Quateman, *Appl. Phys. Lett.* **47**, 239 (1985).

<sup>13</sup>Peter J. Schultz, *Nucl. Instrum. Methods B* **30**, 94 (1988).

<sup>14</sup>Peter J. Schultz and K. G. Lynn, *Rev. Mod. Phys.* (to be published).

<sup>15</sup>S. Valkealahti and R. M. Nieminen, *Appl. Phys. A* **35**, 51 (1984).

<sup>16</sup>A. P. Mills, Jr., and L. Pfeiffer, *Phys. Lett.* **63A**, 118 (1977).

<sup>17</sup>A. P. Mills, Jr., and C. A. Murray, *Appl. Phys.* **21**, 323 (1980).

<sup>18</sup>E. Tandberg, B. Nielsen, G. C. Aers, D. O. Welch, K. G. Lynn, and P. J. Schultz, to be published.

<sup>19</sup>S. M. Sze, *Physics of Semiconductor Devices* (Wiley, New York, 1981), 2nd ed.

<sup>20</sup>R. A. A. Kubiak, W. Y. Leong, M. G. Dowsett, D. S. McPhail, R. Houghton, and E. H. C. Parker, *J. Vac. Sci. Technol. A* **4**, 1905 (1986).

<sup>21</sup>S. Dannefaer and D. Kerr, *J. Appl. Phys.* **60**, 1313 (1986).

<sup>22</sup>S. Dannefaer, *Phys. Status Solidi (a)* **102**, 481 (1987). G. Dlubek and R. Krause, *Phys. Status Solidi (a)* **102**, 443 (1987).

<sup>23</sup>T. E. Jackman, P. J. Schultz, E. Tandberg, and M. W. Denhoff, to be published.

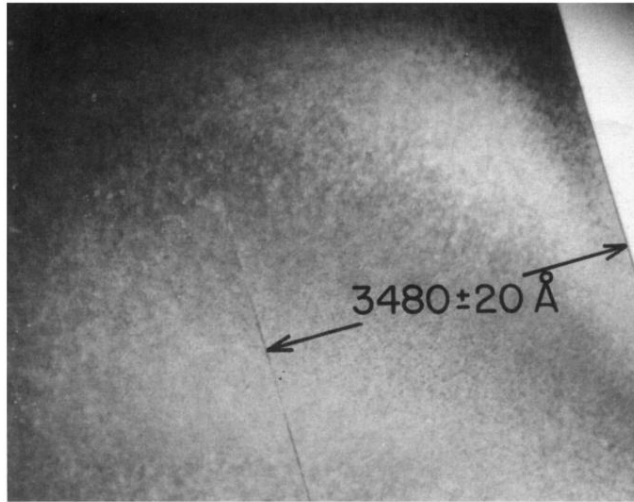


FIG. 3. Transmission micrograph of the Si/Si(100) epilayer of Fig. 2(b). The dark line is due to the oxide-type defects at the interface.